Investigation of Urbach Energy of CdS Thin Films as Buffer Layer for CIGS Thin Film Solar Cell

Priya S. Suryavanshi, C.J. Panchal*

*Applied Physics Department, Faculty of Technology and Engineering,
Vadodara - 390001, Gujarat, India*

CdS (Cadmium Sulphide) has been studied as a buffer layer to form heterojunctions layer with an absorber layer in photovoltaic applications. Different techniques have accounted for deposition CdS layer. We had studied CdS thin film layer by thermal evaporation and chemical bath deposition (CBD) techniques. Structural, optical, electrical and Photoluminescense (Pl) analysis of CdS thin films have been studied. Urbach energy, dark resistivity and light resistivity also have been estimated.

Keywords: Thermal evaporation, CBD, Urbach energy.

1. INTRODUCTION

Cadmium sulphide (CdS) plays key role in various solar cell system such as CdTe, $Cu(In,Ga)Se_2$, $Cu(In,Ga)S$, $Cu_2ZnSnSe_4$. A certified power conversion efficiency of 22.8 % has been recorded for thin film based $Cu(In,Ga)Se_2$ solar cell [1]. Cadmium sulphide is extensively used as n-type semiconducting layer in multi-layered $Cu(In,Ga)Se_2$ solar cell. For p-n junction of solar cell, CdS as a buffer layer have explicit properties such as (a) high transparency, (b) thickness should not be too thick to avoid absorption, nor too thin to avoid short circuit with absorber layer, (c) highly conductive to reduce electrical losses in solar cells and (d) highly photoconductive to not alter the solar cell spectral response [2]. Many different techniques have been accounted for depositing CdS layer. Many researchers had deposited CdS using different techniques such as MOCVD [3], closed space sublimation [4], pulse direct current magnetron [5], combine dip [6], microwave assisted CBD [7], electrodeposition [8], RF-sputtering [9], pulse laser deposition [10], spray pyrolysis [11], screen printing [12], and Chemical vapour deposition [13]. Among all deposition techniques, Chemical Bath Deposition (CBD) technique is found most promising for achieving high efficient solar cell. In present study we have deposited CdS thin films on soda lime glass by two different method (a) thermal evaporation and (b) CBD. In CBD method, conformal coverage of compound takes place.

2. EXPERIMENTAL DETAILS

CdS thin films were deposited by two different techniques, (a) thermal deposition and (b) CBD on soda lime glass substrate. The soda lime glass substrates were organically cleaned by trichloroethylene, acetone and methanol. CdS thin films deposited by thermal evaporation at different substrate temperature (ST) [Room Temperature (RT), 100 °C, 125 °C, 150 °C, 175 °C] with thickness of 50 nm. Pure CdS powder from SIGMA-ALDRICH (99.995 %), USA has been used for thermal deposition. The source to substrate distance was maintained at 8 cm. The substrate temperature was measured by chromel-alummel thermocouple using temperature controller. Rate of Deposition and thickness of thin films deposited by thermal evaporation was estimated by thickness monitor Hind High Vacuum Co. India (HHV DTM-110). Cadmium sulphate ($CdSO_4$), ammonia, thiourea ($SC(NH_2)_2$) were used as initial precursor for depositing CdS by CBD technique. CdS deposited by chemical bath deposition (CBD) with different S/Cd ratio i.e. [1 (sol 1), 2.5 (sol 2), 5 (sol 3), 7.5 (sol 4)]. The cadmium (0.02 M) concentration was kept constant while sulphur concentration was varied i.e. (0.2, 0.5, 1, 1.5 M) pH of bath was maintained to 10. The glass substrate was kept vertical in bath. The solution was continuously stirred to deposit homogenous CdS thin film. Total volume of solution was 100 ml and bath temperature were maintained 65 – 67 °C. The deposition time for CdS thin films was 20 min. Structural, electrical, optical, photoluminescence characterization of CdS thin films deposited by thermal evaporation and CBD technique have studied. Optical parameters such as transmittance, absorption have been measured using UV-Vis spectrometer (300 – 900 nm). Absorption has been calculated using equation (1),

$$\alpha = -\frac{\ln(T)}{d},\qquad(1)$$

where *T* is transmittance of CdS thin films at and *d* is thickness of CdS thin films. Thickness of CdS thin film was 50 nm.

Urbach Energy was also estimate in order to calculate defect energy. Urbach energy is governed by the structural disorder, imperfection in stoichiometric and passivation at the surface. It has been estimated using following equation (2).

Urbach energy was estimated by plotting $ln(\alpha)$ vs energy ($h\upsilon$). The inverse of linear slope is known as Urbach energy (E_U) and 'σ' is the steepness parameter. Dark and light resistivity had been measured using four point probe method. Light resistivity has been measured under white light irradiation source 150 W metal halide lamp. The distance between lamp and CdS thin films was kept 20 cm. Both light and dark resistivity had

---

* cjpanchal_msu@yahoo.com

$$\alpha = \alpha_0 \exp\left[\frac{\left\{\frac{E_g}{kT}\right\}}{\beta}\right] \tag{2}$$

measured using high resistance meter (Keithley 6517B). Indium was used as contact for measuring resistivity.

Photoluminescence analysis of CdS thin film was carried out at room temperature using frequency doubled 532 nm Nd-YAG laser and CCD detector.

X-ray analysis has been carried out using PANalytical X'Pert-Pro (Source: CuK$_\alpha$).

3. RESULT AND DISCUSSION

3.1 Structural Characterization

Structural characterization of CdS thin films deposited by (1) thermal evaporation at different substrate temperature and (2) CBD with different S/Cd ratio have been determined from X-ray analysis. X-ray analysis of CdS thin films deposited by thermal evaporation and CBD techniques are shown in Fig. 1(a) and (b). CdS exhibit two phases i.e. (a) hexagonal and (b) cubic. The preferable phase of CdS for n-type buffer layer to form *p-n* junction with *p* type CIGS is hexagonal. This is because CIGS possess tetragonal phase structure, so in order to avoid lattice mismatch hexagonal phase is preferred rather than cubic. Major peak at 26.7 was observed for CdS thin films which refer to the prime hexagonal phase (002) [14, 15]. At ST 150 °C, the intensity of peak is highest which shows the homogeneous deposition of thin film with stoichiometric composition. No other phase had been found in CdS
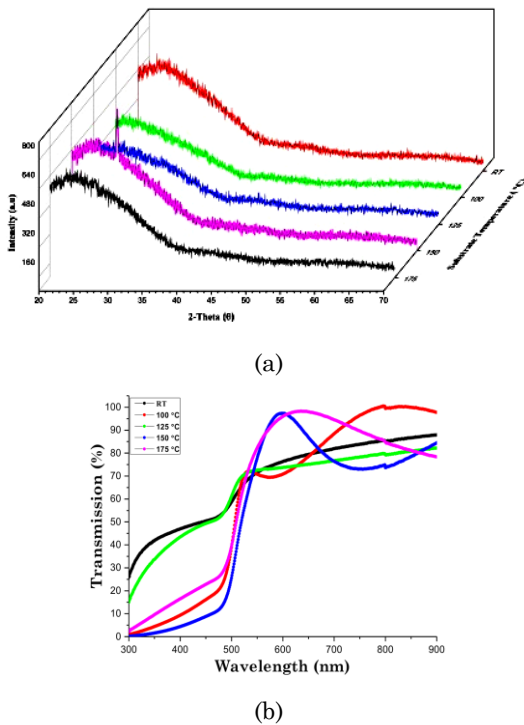

(a)

(b)

Fig.1 – X-ray analysis of CdS thin films deposited by (a) thermal evaporation at different ST and (b) CBD at different

S/Cd ratio

thin films deposited by thermal evaporation. XRD analysis of CdS thin films deposited by CBD technique reflects the presence of other phase also [16, 17]. The hexagonal phase has been confirmed with JCPDS card 41-1049, α-CdS phase.

3.2 Optical Characterization

Optical Characterization is one of the key parameter to analyse the quality of deposited thin films. Transmittance of all CdS thin films deposited by (1) thermal at different ST and (2) CBD at different S/Cd ratio has been measured as shown in Fig. 2.
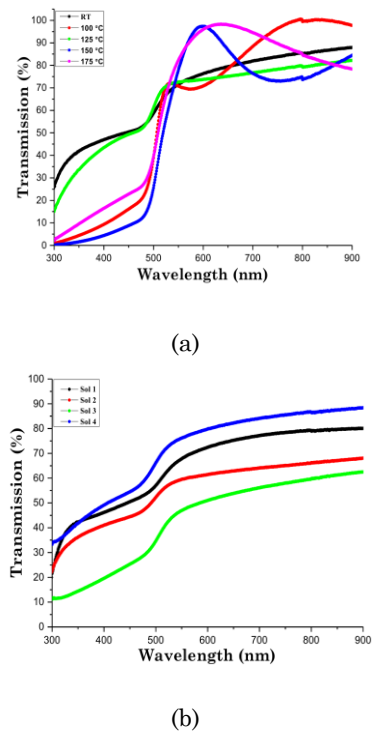

(a)

(b)

Fig. 2 – Transmittance spectra of CdS thin films deposited by (a) thermal evaporation at different ST and (b) CBD at different S/Cd ratio

The average transmittance of CdS thin films deposited at substrate temperature is nearly 75 – 90 % while those films deposited by CBD have transmittance 52 – 74 %. The low transmission of CdS thin film deposited by thermal evaporation at substrate temperature RT, 100 °C, 125 °C, and 175 °C is due to inhomogeneous deposition of CdS thin film. It is also well-known fact that Cd^{+2} adheres faster than S^{-2} ions, due to which large number of defects like vacancies, interstitials, dislocation, strain have been formed during deposition. Due to high vapour pressure and low adhesion of sulphur atoms, stoichiometric composition is not maintained at RT, 125 °C and 175 °C ST. CdS thin film with S/Cd ratio 1 and 7.5 has high transmission. This is due to ion-by-ion growth mechanism which leads to crystal growth. Low transmission in S/Cd ratio 2.5 and 5 is due to colloidal agglomeration cluster formation in the solution. Colloidal aggregates form due to ammonia complex. CdS thin film with S/Cd ratio 7.5 has highest transmission due to less defect density and uniform

coverage of film. Similarly, film deposited at 150 °C ST has homogenous deposition with no pin holes have high transmission. The band gap has been estimated from (absorption coefficient x thickness) vs energy plot is shown in Fig. 3(a) and (b). Band gap of CdS thin films deposited by thermal evaporation is nearly in the range of 2.25-2.34 eV which is in good agreement with bulk CdS (2.42 eV). At 150 °C, substrate temperature band gap is nearly 2.34 eV which is due good crystallinity of the deposited thin films [14, 18]. For CdS thin films deposited by CBD has band gap nearly 2.25 eV with S/Cd ratio 7.5. This indicated higher S/Cd ratio has good crystallinity compare to lower S/Cd ratio. It has been noticed that at higher S/Cd ratio conformal coverage CdS over the glass substrate is good.
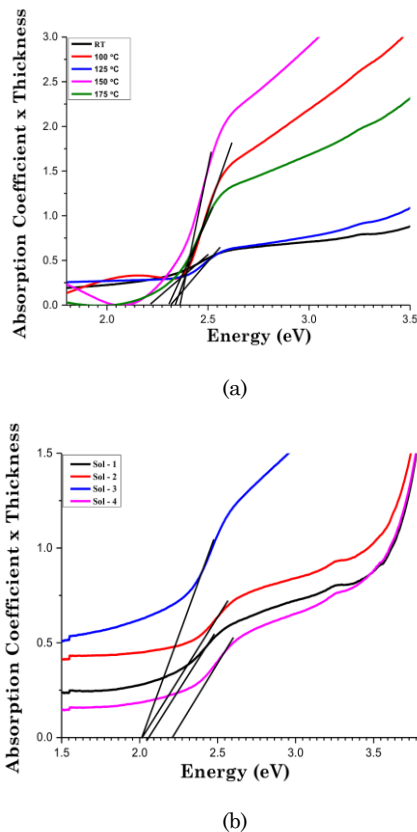

(a)

(b)

Fig.3 – (Absorption coefficient x thickness) vs Energy spectra of CdS thin films deposited by (a) thermal evaporation at different ST and (b) CBD at different S/Cd ratio

The blue shift in band gap energy of CdS thin films from the bulk CdS (2.42 eV) is due to formation of defects. These defects are the traps which affect the optical absorption. The decrease in the optical band gap is due to defect- induced at band tailing. Band tailing below absorption edge is due to formation of location of localized energy states near band edges. It has also been reported that, decrease in optical band gap is due to confinement of charge carrier [18 – 20].

3.3 Urbach Energy and Electrical Characterization

Urbach energy is also known as "band tail width" associated with localised states of amorphous structure in

forbidden gap. Urbach energy is governed by the structural disorder, imperfection in stoichiometric and passivation at the surface [21]. Urbach energy also indicates the disorder of phonon states in the film. Urbach energy 'EU' is found below absorption band edge of compound. The generation of absorption edge at the band gap energy is due to exciton–phonon interaction or may be due to electron–phonon interaction. This can be estimated from steepness parameter. The band bending causes reduction in optical band gap. The higher EU defines the high disorder of phonon states in the films. The high disorder of phonon states in CdS thin films is may be due to thermal disorder or occupancy level of phonon states. The Urbach energy (EU) and steepness parameter (σ) has been estimated for CdS thin film deposited by thermal evaporation and CBD as a function of ST and S/ Cd ratios shown in table 1. It has been found that CdS thin film deposited at 150 °C ST has $E_U = 34.34 \text{ meV}$, while that with S/Cd ratio 5 has $E_U = 54.46 \text{ meV}$. The results indicate that, at RT, 100 °C, 125 °C & 175 °C substrate temperature, high disorder in film is present due to improper stoichiometric composition [22]. For CdS thin films deposited at different S/Cd ratio, at higher S/Cd ratio the disorder decrease, due to uniform deposition of CdS. Some studies on the basis of correlation between Urbach energy open circuit voltage, short circuit current and quantum efficiency [23, 24]. Electrical resistivity of CdS thin films also had been measured and mention in table 2. It has been noticed the change in electrical resistivity of CdS thin film in light and dark condition. The electrical resistivity is in order of $10^5 \ \Omega \cdot \text{cm}$ [14].

Table 1 – Urbach Energy & Steepness parameter for CdS thin films deposited by thermal evaporation & CBD techniques

As grown sample		Urbach Energy (E_U)	Steepness parameter (σ)
At different substrate temperature (°C)	RT	73.52	0.351
	100	43.76	0.590
	125	70.52	0.366
	150	34.44	0.750
	175	55.34	0.467
At different S/Cd ratio	Sol 1	82.98	0.311
	Sol 2	82.03	0.315
	Sol 3	54.46	0.474
	Sol 4	78.74	0.328

Table 2 – Light and Dark resistivity of CdS thin films deposited by thermal evaporation & CBD techniques

As grown sample		Light Resistivity ($10^5_x \Omega \cdot \text{cm}$)	Dark Resistivity ($10^5_x \Omega \cdot \text{cm}$)
At different substrate temperature (°C)	RT	6.86	6.05
	100	6.12	8.64
	125	6.31	12.05
	150	5.31	18.34
	175	5.56	15.52
At different S/Cd ratio	Sol 1	2.72	5.98
	Sol 2	3.41	5.08
	Sol 3	4.46	6.42
	Sol 4	2.03	7.18

3.4 Photoluminescence Analysis

In order to study the defect formation photoluminescence analysis has been carried out. Pl scrutinizes optically active recombination centers. Photoluminescence analysis provide information regarding impurities and defect centres which act as recombination centres for charge carrier which are responsible in degradation of efficiency of solar cell. In CdS material photocurrent is not generated due to radiative or non-radiative recombination, because it contains highly compensated with comparable densities of shallow donors and deep acceptors. Pl analysis of CdS thin films deposited by thermal evaporation and CBD technique has been studied. An emission peak around 1.74 eV has been found in all deposited CdS thin films. Fig. 4(a) and(b) shows the Pl analysis of CdS thin films deposited by thermal evaporation and CBD technique. Peak at energy 1.74 eV is known as 'Red band'. Red band' with energy 1.74 eV is due to sulphur vacancies. Pl intensity of CdS thin films decreases as substrate temperature increase from RT to 150 °C. This indicates that as substrate temperature increase the defect density decreases. But at higher substrate temperature
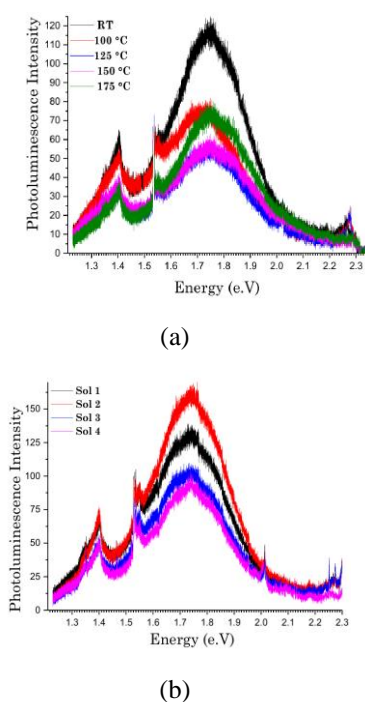

(a)

(b)

Fig. 4 – Photoluminescence analysis of CdS thin films depos-

ited by (a) thermal evaporation and (b) CBD at room temperature

i.e. 175 °C, Pl intensity increased. This increase in Pl intensity is due to increase in defect density [25, 26]. Pl intensity of CdS thin film deposited by CBD technique decreased with the increase in S/Cd ratio. As the concentration of sulphur atoms increase, defect density of sulphur defect decrease. The Pl spectra of CdS thin films deposited by thermal evaporation and CBD technique have gaussian shape which is due to photophysical result of the band measurement of thin film at room temperature. The broadening of shape is due to in-homogenous distribution of cadmium and sulphur atoms and thermal energy associated with it. The Pl emission is not sharpened because of the presence of recombination sites, different impurity concentration is present in grains. It is also noted that red band of CdS thin films is generated due to transition of electrons trapped in surface states to valence band. This type of transition occurs on the formation of crystallographic defect [27].

4. CONCLUSION

N-type buffer layers CdS thin films were deposited on organically cleaned soda lime glass. CdS thin films were deposited using two different techniques i.e. thermal evaporation and CBD. CdS thin films deposited by thermal evaporation at different substrate temperature with thickness 50 nm while CdS thin films deposited by CBD technique at different S/Cd ratios. From the analysis of structural, optical, Urbach energy, electrical and photoluminescence analysis, it has been found CdS thin film deposited at 150 °C shows good crystallinity quality with less Urbach energy. Similarly, thin film deposited by CBD at S/Cd ratio 5, shows result good in agreement with thin film deposited by thermal evaporation technique. In Pl analysis, red band has been observed for thin film deposited at 150 °C and S/Cd ratio 5 with less intensity. This also has been confirmed by Urbach energy estimation.

REFERENCES

1. Philip Jackson, Dimitrios Harriskos, Roland Wuerz, Oliver Kiowski, Andreas Bauer, T.F. Magorian, Michael Powalla *phys. status solidi RRL* **9** No1, 28 (2015).
2. H. Moualkia, S. Hariech, M.S. Aida, *Thin Solid Films* **518**, 1259 (2009).
3. S. Yoon, S. Lee, K. Seo, I. Shim, *Bull. Korean Chem. Soc.* **27** No 12, 2071 (2006).
4. A.I. Oliva, R. Castro-Rodríguez, O Solís-Canto, Víctor Sosa, P.Quintana, J.L. Peña, *Appl. Surf. Sci.* **205**, 56 (2003).
5. F. Lisco, P.M. Kaminski, A. Abbas, K. Bass, J.W. Bowers,

G. Claudio, M. Losurdo, J.M. Walls, *Thin Solid Films* **582**, 323 (2015).
6. Krishnaiah Mokurala, L.L. Baranowski, F.W. de Souza Lucas, Sebastian Siol, Maikel F.A.M van Hest, Sudhanshu Mallick, Parag Bhargava, Andriy Zakutayev, *ACS Comb. Sci.* **18**, 583 (2016).
7. J. Ma, S.Das, C. Lu, *RSC Adv.* **6**, 107886 (2016).
8. M. Fathy, A. Kashyout, S. Yamny, *Int. J. Electrochem. Sci.* **9**, 6155 (2014).
9. J. Choi, S.Jung, C.Chung, *J. Korean Phys. Soc.* **68** No 3, 425 (2016).

10. M. Sanz, R. Nalda, J. Marco, *J. Phys. Chem. C* **114**, 4864 (2010).
11. V. Popescu, H. Na'cu, *Chalcogenide Lett.* **3** No9, 67 (2006).
12. V. Klaďko, O. Lytvyn, P. Lytvyn, *Semicon. Phys. Quant. Electron. Optoel.* **5** No2, 170 (2002).
13. Y. Sánchez, M. Rodríguez, H. Xie, *Sol. Energy Mater. Sol. C.* **158**, 138 (2016).
14. N.M. Shah, J.R. Ray, M.S. Desai, C.J. Panchal, *J. Opt. Adv. Mater.* **12** No10, 2052 (2010).
15. L. Huang, Z. Wei, F. Zhang, X. Wu, *J Alloy. Compd.* **648**, 591 (2015).
16. S. Jassim, A. Zumaila, G Waly, *Results Phys.* **3**, 173 (2013).
17. W. Kumarage, L. Wijesundara, V. Seneviratne, *Proc. Engin.***139**, 64 (2016).
18. B. Singh, J. Singh, J. Kaur, *Physica B* **490**, 49 (2016).
19. H. Pushpalatha, S. Bellappa, T. Narayanswamy, *J Alloy. Compd.* **648**, 591 (2015).
20. A. Slonopas, H. Ryan, B. Foley, *Mater. Sci. Semicon. Proc.* **52**, 24 (2016).
21. I. Studenyak, M. Kranjčec, M. Kurik, *Int. J. Opt. Appl.* **4** No 3, 76 (2014).
22. M. Islam, M. Hossain, M. Aliyu, *Energy Procedia* **33**, 203 (2013).
23. M. Solomon, A. Johnson, *Elements: Boston College Undergraduate Res. J.* **11** No1, 7896 1 (2015).
24. M. Troviano, K. Taretto, *EU PVSEC Proceedings of 24th European Photovoltaic Solar Energy Conference 21-25 September 2009, Hamburg, Germany*, 2933 (2009).
25. F. Gemain, I. Robin, S.Renet, *phys. status solidi c* **9** No8–9, 1740 (2012).
26. R. Prabhu, M. Khadar, *Bull. Mater. Sci.* **31** No3, 511 (2008).
27. J. Andez, G. Puente, A. Acevedo, *Semicond. Sci. Technol.* **18**, 111 (2003).